ACS OMEGA

Article

Cite This: ACS Omega 2019, 4, 1781−1790

http://pubs.acs.org/journal/acsodf

Processing-Mediated Different States of Dispersion of Multiwalled Carbon Nanotubes in PDMS Nanocomposites Influence EMI Shielding Performance

Harsha Nallabothula,[†] Yudhajit Bhattacharjee,[†] Laxmi Samantara,[‡] and Suryasarathi Bose*[,†]

[†]Department of Materials Engineering, Indian Institute of Science, Bangalore 560012, India

[‡]Corporate Research and Development Centre, Momentive Performance Materials Pvt. Ltd, Survey #9 Electronic City West (Phase 1), Bangalore 560100, India

ABSTRACT: Advancement in wireless technology has increased the usage of wireless devices extensively in the past few years, which led to an increase in electromagnetic interference (EMI) in the environment. Extensive research on fabrication of EMI shielding materials has been done. However, the role of processing method of polymer composites in EMI shielding has been neglected. In this work, we investigate the role of two polymer processing methods, spin coating and compression molding, in EMI shielding application. Poly(dimethylsiloxane) (PDMS) nanocomposites with multiwalled carbon nanotube (MWCNT) were spin-coated onto glass slides and compression-molded to a similar thickness. The processing method that exhibited the best shielding was employed to fabricate multiple PDMS composites comprising different compositions of MWCNT and Fe_3O_4 and stacked to form a multilayered EMI shielding PDMS composite. Scanning electron micrographs revealed that MWCNT in spin-coated composites are significantly more agglomerated than in the compression-molded film. Direct current conductivity and curing temperature were higher in compression-molded films as the filler formed a well-percolated network and hindered cross-linking of polymer chains. EMI shielding results revealed that spin-coated films demonstrated greater shielding effectiveness than compression-molded composites in the Ku-band (12−18 GHz). Individual agglomerates of MWCNT in spin-coated film attenuated incoming electromagnetic radiation more effectively than well-dispersed MWCNT in compression-molded films. Therefore, PDMS composites of different compositions of MWCNT and Fe_3O_4 nanoparticles were prepared through spin coating and stacked with a gradient of filler concentration, which resulted in maximum shielding of −28 dB, i.e., shielding more than 99% of incoming EM radiation by a 0.9 mm film.

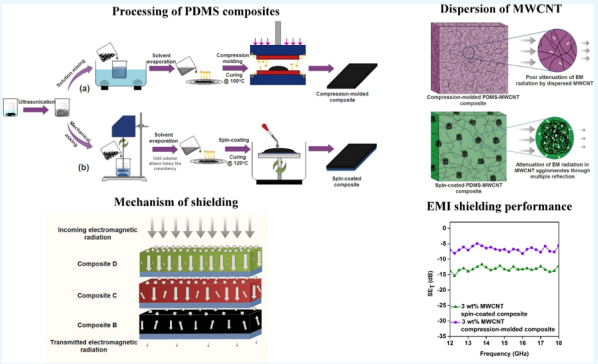

INTRODUCTION

With the advent of wireless electronics and rapid growth in electronics and communication, interference of electromagnetic waves can no longer be neglected. Recent technological advancements have led to the use of a wide range of radio frequencies for reliable performance of wireless devices and miniaturization of electronic components, making electrical devices more compact every year. Hardware−software interfacing through concepts such as Internet of Things promotes the use of wireless communication in everyday life and advancement in mass production of electronic devices, making it affordable to the masses. All of these advancements have led to the use of high-energy electromagnetic (EM) radiation, which interferes with EM radiation from other devices, increasing electromagnetic interference (EMI) in our environment. Interference of EM radiation with electronic components can lead to malfunction, data loss, or complete impairment of the device.[1−3] Although there have not been conclusive reports on the effects of EMI on human beings, World Health Organization and International Agency for Research on Cancer have classified radio frequency EM fields as possibly carcinogenic and increasing the risk of malignant brain cancer and glioma.[4] Several measures have been taken since the 20th century to reduce EMI through allocation of specific bands of EM radiation and electromagnetic compatibility of electronic devices, which is primarily through the shielding of the device of interest.[5]

Shielding electronic components with metals has been an old but effective method in shielding EM radiation through reflection. Mobile carriers in metals absorb EM radiation and release it in all directions, resulting in scattering and a minuscule attenuation of incident radiation.[6] As metals have abundant mobile carriers, they are known to be the best EMI shielding materials and are still used for EMI shielding in commercial electronic devices. However, their corrosive nature, poor processability for encapsulation of miniaturized components, and high cost had made polymer composites a better candidate for EMI shielding. As polymers are mostly

Received: October 24, 2018
Accepted: December 14, 2018
Published: January 22, 2019

DOI: 10.1021/acsomega.8b02920
ACS Omega 2019, 4, 1781−1790

insulators and poor EMI shielding materials, EMI shielding particles are added to the polymer. The low cost, easy processability, and reusability of polymers, compounded with the excellent magnetic, dielectric, and conducting properties of filler materials, result in EMI shielding materials with good shielding properties and industrial viability. Composites of acrylonitrile butadiene styrene, polystyrene, polyethylene, poly(vinylidene flouride), etc. with multiwalled carbon nanotube (MWCNT), graphene, ferrites, iron, mu-metal, and mxene have been fabricated, some of which exhibit shielding similar to metals.[7−10]

The extent of electromagnetic shielding exhibited by any material is analyzed by measuring the transmission of electromagnetic waves through the material termed as total shielding effectiveness (SE_T) expressed in decibels (dB). The theory of EMI shielding was first developed by Schelkunoff, based on transmission line concepts of reflection and transmission.[11] The original model explained shielding in homogeneous materials, which has been modified to explain EMI shielding in heterostructures like multilayered, porous, and composite materials.[12−14] The total shielding (SE_T) by any material can be differentiated into three factors as shielding through reflection/scattering (SE_R), absorption (SE_A), and multiple internal reflection (SE_M). SE_M can be neglected when total shielding is more than 10 dB.

$$SE_T = SE_R + SE_A + SE_M$$

The different forms of shielding effectiveness can be calculated from vector network analyzer (VNA) using scattering parameters as follows

$$SE_T = 10 \log\left(\frac{P_t}{P_i}\right) = 10 \log_{10} \frac{1}{|S_{21}|^2}$$

$$SE_R = 10 \log_{10} \frac{1}{1 - S_{11}^2}$$

$$SE_A = 10 \log_{10} \frac{1 - S_{11}^2}{S_{12}^2}$$

where S_{ij} are the scattering parameters, which can be deduced from transmission and reflection coefficients of the material. Here, SE_R is a complex function of intrinsic impedance and SE_A is a function of propagation constant of the material. To shield primarily through absorption of EMI, the shielding material should show low impedance mismatch with air and high propagation constant. Materials with permanent dipoles like magnetic, dielectric, semiconductor, piezoelectric, ferroelectric materials, etc. can absorb EMI. Polymer composites with these fillers would exhibit excellent EMI shielding through absorption. However, incorporation of the above-mentioned materials alone in the polymer typically results in very low shielding as the entire system lacks electrically percolation. Hence, a conducting network is essential to shield EM waves through either reflection or absorption, which results in a net shielding through scattering/absorption of EM waves.

While metals can be incorporated into the polymer matrix for the formation of an electrically percolated network, carbonaceous materials like carbon nanotubes and graphene stand as better alternatives for the formation of conducting network in the polymer composite.[15] The low density, high aspect ratio, high conductivity, and abundant functional groups on the surface make MWCNT, graphene, graphene oxide, and other carbonaceous materials prime candidates for polymer nanocomposites. Magnetic particles have been frequently used along with conducting materials in polymer composites to improve absorption of EM radiation. Iron, iron oxide, and ferrites like cobalt, manganese, and nickel are some of the materials studied extensively and shielding mostly through absorption. Elastomeric EMI shielding materials are useful in niche applications; however, research has not been extensive compared to other polymers. High elasticity, chemical inertness, and wide operational temperatures of silicone polymers make them prime materials for diverse environments.[16−18] Under the framework of existing research on elastomeric EMI shielding materials are silicones such as commonly used poly(dimethylsiloxane) (PDMS), which has been used mostly for structural integrity of EMI shielding architecture.[3,19−22]

As most of the research was focussed on fabricating the best EMI polymer composites, the effect of different processing methods on EMI shielding has not been extensive. Dispersion of filler material, morphology of blends, and polymer−filler interaction can be tailored through the processing method employed. It governs the mechanical, electrical, thermal, and other properties and EMI shielding.[23−26] However, study of the effect of processing on EMI shielding has been scant.[27−29] Alper et al. compared solution mixing with ultrasonication and melt mixing of polyurethane composites.

While the choice of filler dictates the extent of shielding, with the use of appropriate design and architecture comprising different fillers, shielding can be improved. Selective localization of magnetic and conducting fillers in blends, foams, layer-by-layer stacking, etc. is one of the few methods commercially being employed.[9,15,30] Multilayered stacking using alternate conducting and absorbing layers, concentration and thickness gradient, etc. have shown excellent shielding compared to single composition composites of the same thickness.[31,32]

In this work, the role of processing method on EMI shielding was studied. PDMS−MWCNT composite thin films were fabricated through spin coating and compression molding. Composites fabricated by these processing methods were studied to understand the cause for difference in SE_T through characterization of the composites for electrical conductivity, dispersion of MWCNT, etc. The better processing method was employed to fabricate PDMS composites of Fe_3O_4 and MWCNT of different concentrations for construction of multilayered architecture of PDMS composites with a gradient in the concentration of fillers, which exhibited excellent SE_T.

CHARACTERIZATION

Fe_3O_4 particles were characterized through FEI Technai F30 transmission electron microscopy (TEM) at an accelerating voltage of 300 kV, and X'Pert Pro powder XRD system from PAN analytical was used for determining the crystal structure, and Lakeshore Vibratory Sample Magnetometer (VSM) was used for determining the magnetic properties at room temperature with an applied force of −2000−2000 Oe.

Scanning electron micrograph of cryofractured PDMS composites was obtained using Carl Zeiss and ULTRA 55 field emission scanning electron microscope at an accelerating voltage of 5 kV.

Thickness of the composites was measured using a Leica Optical microscope DM 2500-M by fixing the thin film

DOI: 10.1021/acsomega.8b02920
ACS Omega 2019, 4, 1781−1790

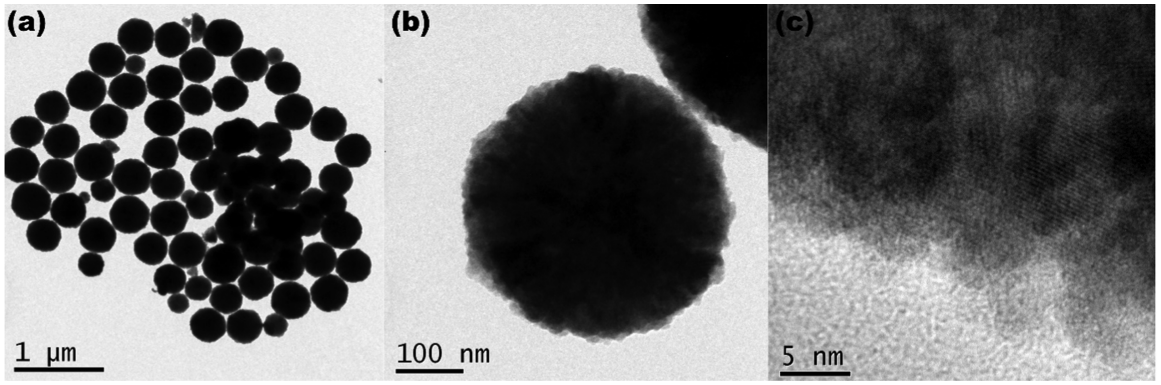

Figure 1. (a, b) Transmission electron micrographs of Fe_3O_4 nanoparticles at different magnification levels. (c) HRTEM images of Fe_3O_4 depicting polycrystallinity.

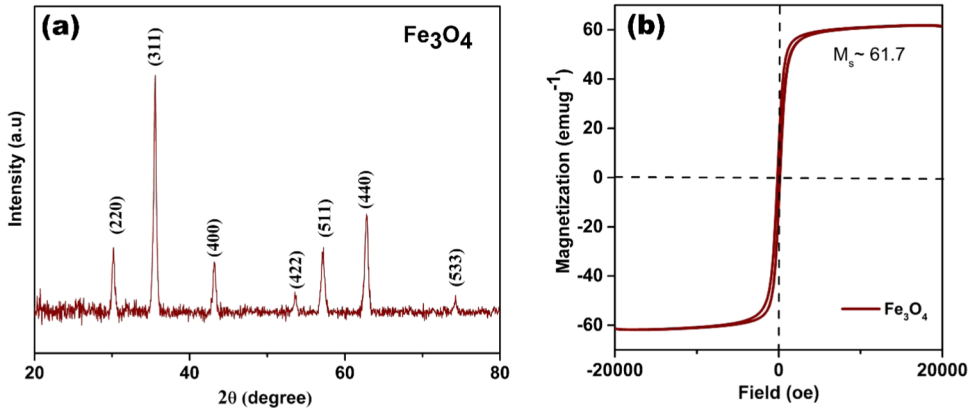

Figure 2. (a) XRD pattern of synthesized Fe_3O_4 nanoparticles. The peaks confirm that Fe_3O_4 has cubic lattice. (b) Vibrating sample magnetometer plot of Fe_3O_4 showing high-saturation magnetization of 61.7 emu/g.

vertically under the objective lens and measuring across the cross section of the film.

Dirrect current (DC) conductivity of the thin films was measured through the van der Pauw method by calculating the sheet resistance using Agilent b1500 a semiconductor device analyzer.

Curing temperature of the thin films was measured using Discovery hybrid rheometer by TA Instruments. PDMS composite was placed between parallel-plate geometry of 1 mm gap at a strain rate of 0.1 s^{-1}, a temperature ramp rate of 5 °C/min from 30 °C, and an angular frequency of 1 rad/s.

The mechanical properties of the thin-film composites were characterized through nanoindentation using Hysitron TI 900 Tribo Indenter with a spherical indenter. A dwell time of 10 s and a constant load of 10 μN were used.

EMI shielding effectiveness (SE) of the polymer composites was measured using an Anritsu VNA MS4642A in the X-band region (12−18 GHz).

RESULTS AND DISCUSSION

Characterization of Fe_3O_4 Nanoparticles. Materials with magnetic and electric diploes typically absorb EM radiation and reduce the release of EM radiation into the environment compared to conducting particles, which reflect EM radiation back into the atmosphere. Ferromagnetic Fe_3O_4 nanoparticles were synthesized through the hydrothermal process and used as an EM absorber in PDMS composites. The morphology of Fe_3O_4 nanoparticles was characterized using bright-field transmission electron microscopy techniques, as presented in Figure 1. Figure 1a of Fe_3O_4 nanoparticles confirm spherical morphology with size varying between 400 and 600 nm and indicating that each nanoparticle is polycrystalline, comprising fine grains of Fe_3O_4, which can be seen in Figure 1c. Crystal structures of Fe_3O_4 nanoclusters were further analyzed through X-ray diffraction. In Figure 2a, X-ray diffraction pattern system confirms the spinel structure of Fe_3O_4 and the peaks (220), (311), (400), (422), (511), (440), and (533) were identified and match the peaks of fcc lattice (JCPDS no. 88-0866). Magnetic hysteresis of Fe_3O_4 nanoparticles was obtained through room-temperature VSM (Figure 2b), showing a coercivity of 154 Oe, remnant magnetization of 11.4 emu g^{-1}, and saturation magnetization (MS) of 61.7 emu g^{-1} depicting its strong magnetization characteristics.

Dispersion of MWCNT in PDMS Composites. Properties of polymer composites can often be controlled by the processing method employed. It determines the dispersion of filler in the polymer, localization of fillers in case of blends, chemical interaction between polymer and filler, etc., which consecutively determines elasticity, brittleness, electrical conductivity, SE, and several other properties of the polymer composites. In the realm of EMI shielding, the state of fillers determines the extent of shielding as most of the polymers are insulators, which can be characterized through electron microscopy. To understand the role of processing in EMI shielding, PDMS composites comprising 3 wt % MWCNT have been spin-coated onto a glass substrate and compression-molded to produce spin-coated and compression-molded thin

DOI: 10.1021/acsomega.8b02920
ACS Omega 2019, 4, 1781−1790

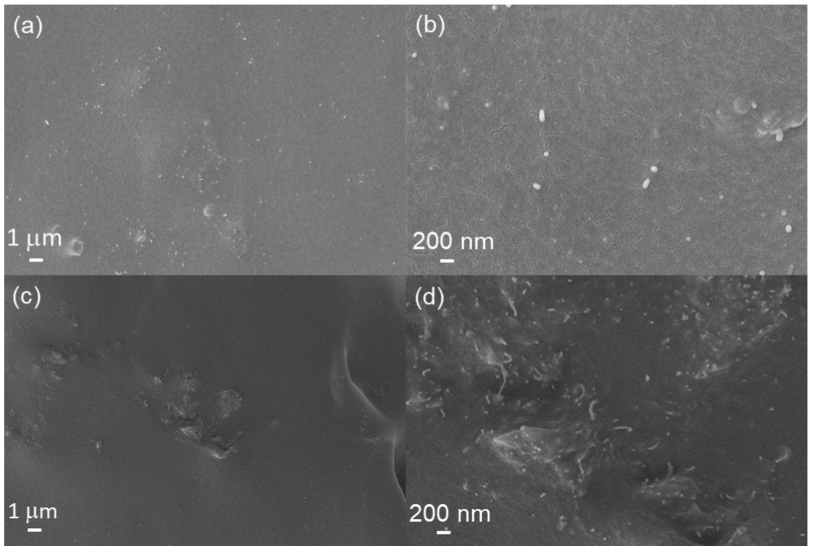

Figure 3. SEM images of 3 wt % MWCNT PDMS composite thin films processed through (a, b) compression molding and (c, d) spin coating. MWCNTs are well dispersed in compression-molded film, while agglomerates of MWCNT are seen in spin-coated film.

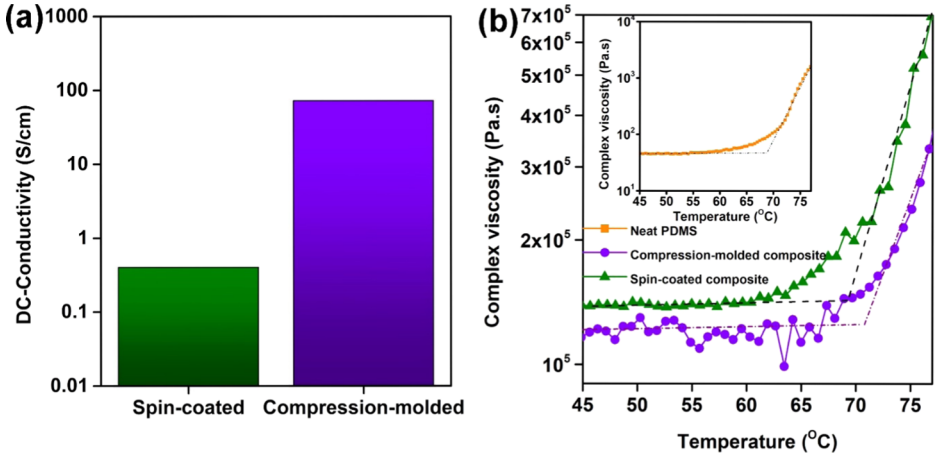

Figure 4. (a) DC conductivity of spin-coated and compression-molded films. Although the spin-coated film exhibited lower DC conductivity compared to the compression-molded film, it exhibited a well-percolated network of MWCNT as it showed a conductivity of 0.4 S/cm. (b) Complex viscosity of neat PDMS and PDMS−MWCNT composites processed through compression molding and spin coating across a temperature range to identify gelation point (onset of curing temperature). Neat PDMS began curing earlier than PDMS−MWCNT composites and spin-coated composite cured earlier than compression-molded composite as MWCNTs are agglomerated in spin-coated composite and absorb heat poorly compared to well-dispersed MWCNT in compression-molded composite.

films, respectively. The thin films were cryofractured and imaged using scanning electron microscopy. SEM images of these composites in Figure 3 showed that MWCNTs are well dispersed in compression-molded films, compared to spin-coated films, which have large agglomerates of MWCNT. The presence of agglomerates in spin-coated films can be attributed to the difference in processing conditions of the composites, as mechanical mixing does not disperse MWCNT completely compared to ultrasonication.

DC Conductivity of PDMS Composites. Electrical conductivity is a necessary criterion for a material to exhibit EMI shielding, through either reflection or absorption. An electrical percolation in a polymer composite is paramount for EMI shielding. However, improved electrical conductivity in a composite does not imply an improvement in shielding because conductivity assists in shielding indirectly through formation of an electrical network, while the filler material attenuates EM radiation.[6,33,34] DC conductivity of spin-coated and compression-molded thin films was measured through the van der Pauw method. As shown in Figure 4a, well-dispersed compression-molded film exhibited a conductivity of 7.2×10^{1} S/cm, while the spin-coated composite exhibits 4.1×10^{-1} S/cm, nearly 2 orders of magnitude lower than the compression-molded film. It is envisaged that the spin-coated composite show lower electrical conductivity due to the presence of agglomerates. However, the conductivity of spin-coated composite is substantial enough to accept that a well-percolated network off MWCNT and the agglomerates exists in the composite film. As we know that conductivity increases with frequency of applied voltage, in GHz range, both the films are expected to have similar electrical conductivity, even though they exhibited different SE.

$$\sigma_{AC}(\omega) = \sigma_{DC} + A\omega^{n}$$

where ω is the angular frequency, σ_{DC} is the direct electrical conductivity, A is the temperature-dependent constant, and n

DOI: 10.1021/acsomega.8b02920
ACS Omega 2019, 4, 1781−1790

is the exponent. The exponent is the measure of the three-dimensional (3D) network of capacitor or resistor and depends on both frequency and temperature, and the value is in the range of 0−1. Hence, electrical conductivity must be used to determine the extent of percolation in the system only.

Curing of PDMS Composites. Addition of fillers affects polymer properties like mechanical strength, viscosity, etc. Although the effects are favorable in some properties, they can be also detrimental, especially on processing properties such as viscosity, T_g, etc., which control energy consumption during manufacturing. The effect of processing methods on curing of PDMS−MWCNT composites is studied through rheology of uncured PDMS composites. Complex viscosity of PDMS composites processed through spin coating and compression molding was measured from 40 to 80 °C. An increase in viscosity indicated the onset of curing, which can be seen in Figure 4b. Both spin-coated and compression-molded composites showed very high viscosity compared to neat PDMS due to the presence of MWCNT, which hinder the motion of polymer chains. The onset of curing was higher in the composites with MWCNT as it hinders cross-linking through absorption of heat by MWCNT. The curing temperatures of compression-molded composite and spin-coated composite are similar, indicating that the processing method did not influence the curing kinetics of the composites.

Mechanical Properties. Mechanical properties are essential for understanding the application of the materials in different environments, durability, and their life time. As the spin-coated composite film is adhered to a glass substrate, which cannot be separated, it limits the extent of characterization for mechanical properties to surface characterizations. Hardness of the composites was measured through nano-indentation using a spherical indenter at a constant load of 10 μN. Table 1 shows the surface hardness and reduced modulus of the spin-coated and compression-molded composites to be on the order of mega pascals. PDMS being an elastomer exhibits low hardness, which was marginally increased by the addition of MWCNT. From Table 1, we see that the compression-molded composite exhibits better hardness compared to the spin-coated composite due to relatively better dispersion of MWCNT. However, the spin-coated composite shows greater deviation compared to the compression-molded composite, which can be attributed to the presence of agglomerates of MWCNT, which produce higher hardness compared to the matrix (PDMS in this context) when the indenter indents the agglomerates.

Table 1. Hardness and Reduced Modulus of Different PDMS Composites

type of composite	load (μN)	hardness (MPa)	reduced modulus (MPa)
spin-coated	10	8.36 ± 3.01	10.10 ± 4.30
compression-molded	10	11.48 ± 0.54	8.48 ± 1
neat PDMS	10	7.24 ± 0.07	5.05 ± 0.1

EMI Shielding of PDMS Composites. The effect of processing method on EMI SE was studied comparing SE of spin-coated and compression-molded thin films. PDMS composite thin films comprising 3 wt % MWCNT were fabricated through spin coating and compression molding. Spin-coated composite film was fabricated on a glass substrate and used along with the substrate for all of the characterizations, as the thin film adhered strongly to the substrate while compression-molded film was a free-standing thin film. However, the glass substrate did not contribute to SE_T, which was verified by measuring SE of plain glass slide, compression-molded film along with the glass substrate, and free-standing compression-molded film, as shown in Figure 5a. We saw that the glass substrate showed zero dB of shielding and SE_T values of both the free-standing film and the glass substrate were very similar, implying that the glass substrate did not contribute to SE_T. SE_T values of spin-coated and compression-molded films were measured as shown in Figure 5b. The compression-molded composite despite being 30 μm thicker than spin-coated film showed −7.5 dB of shielding, while the spin-coated film showed −13.5 dB. Hence, we propose that agglomerates of MWCNT in spin-coated film are assisting in shielding. DC conductivity of the composite films showed that the compression-molded film exhibited higher conductivity but shielded poorly compared to the spin-coated film. The spin-coated film exhibited a conductivity of 0.4 S/cm, and such a magnitude of electrical conductivity is possible only if it contains a percolated network. The agglomerates of MWCNT appear to behave as attenuating sites in the polymer composite, which are electrically connected to each other forming an electrically percolated network of MWCNT agglomerates. When an electromagnetic wave passes through both the composites, it gets attenuated significantly when it encounters agglomerates of MWCNT compared to interacting with several individual MWCNTs. Hence, the difference in shielding in these composite films was due to the difference in frequency of interaction of the incident electromagnetic wave with MWCNT as it propagated through the composite. This clearly demonstrates that despite having the same filler content, the polymer composites exhibited discrete EMI shielding performances, demonstrating the effect of polymer processing method on EMI shielding performance.(Figure 6)

While spin coating is a lab-scale process, composites processed through this method exhibited better shielding compared to compression-molded composites, which is a well-established industrial process for manufacturing on a commercial scale. Spin coating has been employed for the fabrication all of the composites here off as it gives better shielding. PDMS composite thin films with different compositions of Fe_3O_4 and MWCNT were fabricated through spin coating to achieve higher SE primarily through absorption (Table 2). Fe_3O_4 has been extensively studied as EMI shielding material, shielding primarily through absorption. Table 3 comprises PDMS composites fabricated through spin coating with varied composition of fillers, their thickness, and SE_T. While it is known that addition of magnetic particles improves SE_T from Figure 7a and Table 3, we see that SE_T of composites with magnetic particles was less than SE_T of composites without magnetic particles because addition of magnetic particles improves shielding through absorption and does not improve the total shielding. From Figure 7a, we see that PDMS−Fe_3O_4 composites without MWCNT showed zero shielding due to the absence of an electrically percolated network, which implies that electrical percolation is one of the necessary conditions for shielding. Multilayered PDMS composites were fabricated through physical stacking of spin-coated composites. Multilayered composites typically show better shielding due to increased attenuation of EM waves through impedance mismatch at the interface of two films. A greater impedance mismatch increases the reflectance of EM

DOI: 10.1021/acsomega.8b02920
ACS Omega 2019, 4, 1781−1790

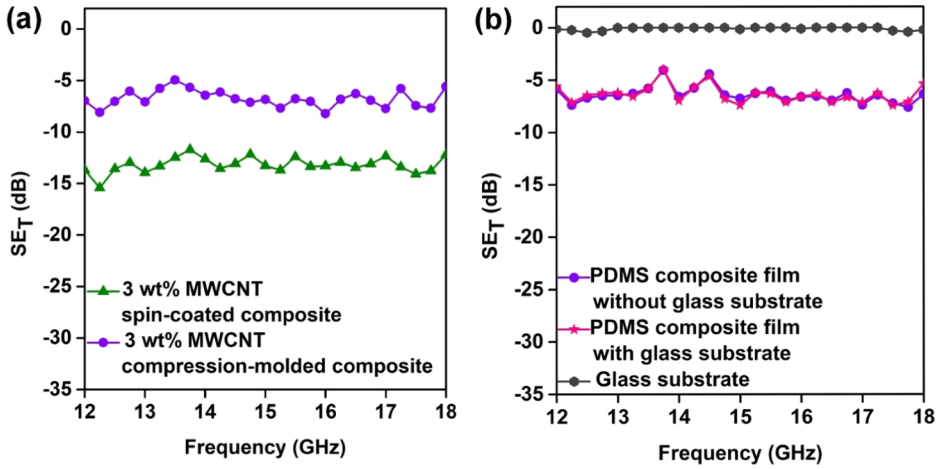

Figure 5. (a) SE$_T$ of 3 wt % MWCNT PDMS composite film processed through compression molding, glass substrate, and compression-molded film along with glass substrate to check the effect of glass substrate on EMI shielding. The plain glass substrate showed negligible shielding and stacking along with a compression-molded film that did not change SE$_T$ of the glass film system, indicating that the glass substrate did not contribute to shielding (b) SE$_T$ of 3 wt % MWCNT PDMS composite thin film processed through compression molding and spin coating. The spin-coated sample showed an average shielding of −13.5 dB, while the compression-molded film showed −7 dB. The thickness of the spin-coated film was 150 μm, while the thickness of the compression-molded film was 180 μm. The compression-molded film, despite being 30 μm thicker than the spin-coated film, exhibited poor shielding.

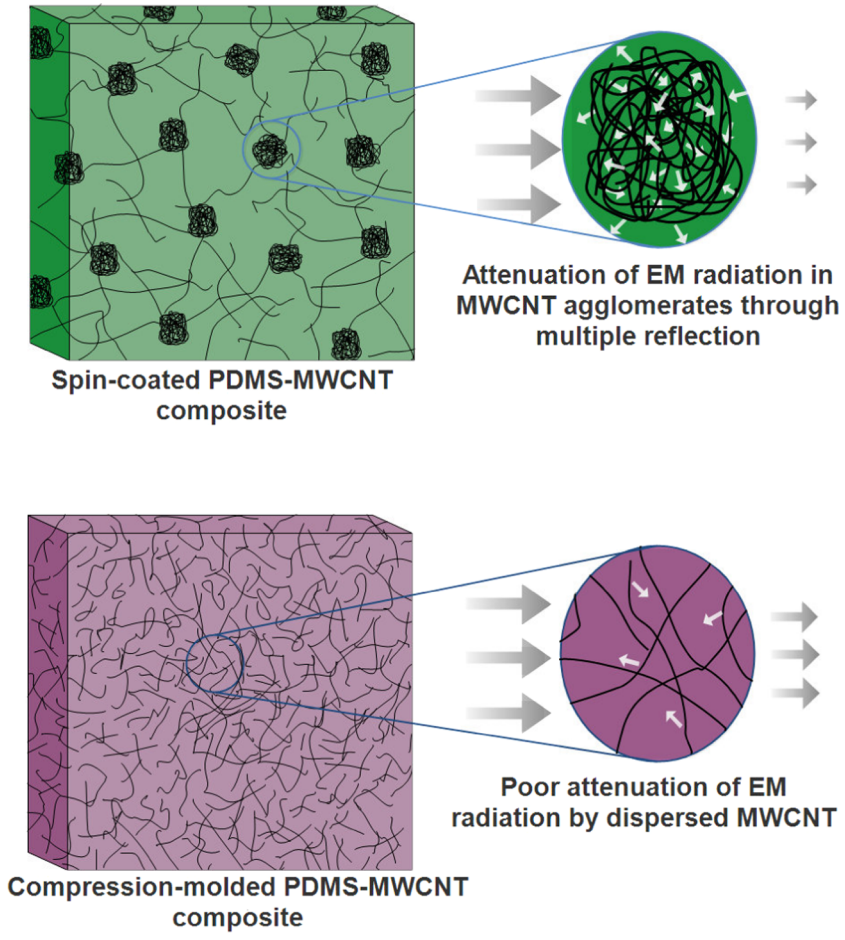

Figure 6. Schematic illustrating the mechanism of shielding in spin-coated and compression-molded composites. The agglomerates in spin-coated composite attenuate EM radiation extensively through extensive interaction of EM radiation with MWCNT due to dense packing in the agglomerates. The attenuation is less in compression-molded films due to reduced interaction of EM radiation with MWCNT.

waves into the composite resulting in improved attenuation of the EM wave before it propagates through the multilayered stack. Three multilayered composites were fabricated using different compositions with a gradient in concentration of filler as mentioned in Table 4, having a thickness of 900 μm. These multilayered composites exhibit SE$_T$ in 20−28 dB range, which

DOI: 10.1021/acsomega.8b02920
ACS Omega 2019, 4, 1781−1790

Table 2. Comparison of PDMS Composite Thin Films

type of composite	DC conductivity (S/cm)	curing temperature (°C)	thickness (μm)	SE_T (dB)
spin-coated	0.4	69	150	−13.6
compression-molded	72	71	180	−7.5
neat PDMS	10^{-12}	68	1000	0

Table 3. Composition of PDMS Composite Films and SE_T

composite name	filler material	composite thickness (μm)	SE_T (dB)
A	1 wt % Fe_3O_4	200	0
B	0.5 wt % MWCNT	150	−2
C	1.5 wt % MWCNT	150	−7.5
D	3 wt % MWCNT	150	−13.5
E	1 wt % Fe_3O_4 + 1 wt % MWCNT	300	−6.5
F	5 wt % Fe_3O_4 + 3 wt % MWCNT	300	−10.5

is equivalent to shielding more than 99% (>−20 dB) of incoming radiation, as seen in Figure 7b. The total shielding effectiveness achieved through multilayered stacking is one of the best results in the literature, as shown in Table 5, which compares average SE_T of PDMS composite thin films from the literature with the current work (Figure 6, Table 2, and Figure 8).

CONCLUSIONS

The effect of processing method on EMI shielding was investigated by processing PDMS−MWCNT composites through compression molding and spin coating. Agglomerates of MWCNT electrically percolated in spin-coated composite showed better attenuation of EM radiation compared to well-dispersed MWCNT in compression-molded composite. This concludes that, despite exhibiting high DC conductivity, compression-molded composite shielded poorly compared to spin-coated composite. The effect of glass substrate has been studied, and it was concluded that it did not contribute to SE_T although it was dielectric in nature. While addition of Fe_3O_4 reduced SE_T of the composite, from previous research work on Fe_3O_4, it was concluded that percent absorption of EM radiation had increased. Ultimately, stacks of different PDMS composites across the concentration gradient resulted in a maximum SE_T of −28 dB, which is equivalent to blocking nearly 99.9% (~30 dB) of incoming EM radiation.

Table 4. Composition and SE_T of Multilayered Composites

multilayered composite	composites used	SE_T (dB)	composite thickness (μm)
X	D−C−B−B−C−D	−26	900
Y	F−D−C−E	−21	900
Z	D−E−C−F	−23	900

EXPERIMENTAL SECTION

Materials. Vinyl-terminated linear poly(dimethylsiloxane) (PDMS) (viscosity, 65 Pa s) and curing agent comprising hydrogen siloxane fluid, Pt-curing catalyst, and inhibitor were kindly provided by Momentive performance materials. MWCNT was purchased from Nanocyl, NC7000 (average diameter: 9.5 nm; average length: 1.5 μm). Tetrahydrofuran (THF), ethylene glycol, dichloromethane (DCM), sodium acetate (CH_3COONa), and sodium carbonate (Na_2CO_3) were purchased from S D Fine-Chem Limited. Poly(ethylene glycol) (PEG-4000) was purchased from SRL Chemicals, and $FeCl_3 \cdot 6H_2O$ was purchased from Thomas Baker.

Fe_3O_4 Nanoparticle Synthesis. Fe_3O_4 nanoparticles were synthesized through hydrothermal method.[40] $FeCl_3 \cdot 6H_2O$ (6 mmol) was dissolved in 40 mL of glycol. Further, 1 g of PEG-4000 and 43 mmol sodium acetate was added to the solution and stirred vigorously for 30 min. The mixture was then transferred into a Teflon autoclave and placed in a hot-air oven at 200 °C for 24 h. A black precipitate was collected with a permanent magnet, washed with ethanol, distilled water several times, and finally dried in a vacuum oven at 100 °C.

Composite Preparation. MWCNTs were dispersed in THF through probe sonication for 15 min, followed by bath sonication for 15 min. Fe_3O_4 nanoparticles were also dispersed in THF through bath sonication. The solutions were mixed and sonicated for 45 min to ensure homogeneous dispersion of the particles. In composite where Fe_3O_4 was not included, MWCNT was further sonicated for 45 min to ensure equivalent sonication time of filler materials in all of the composites.[41] PDMS added to the solution was processed as shown below for compression molding and spin coating (Figure 9).

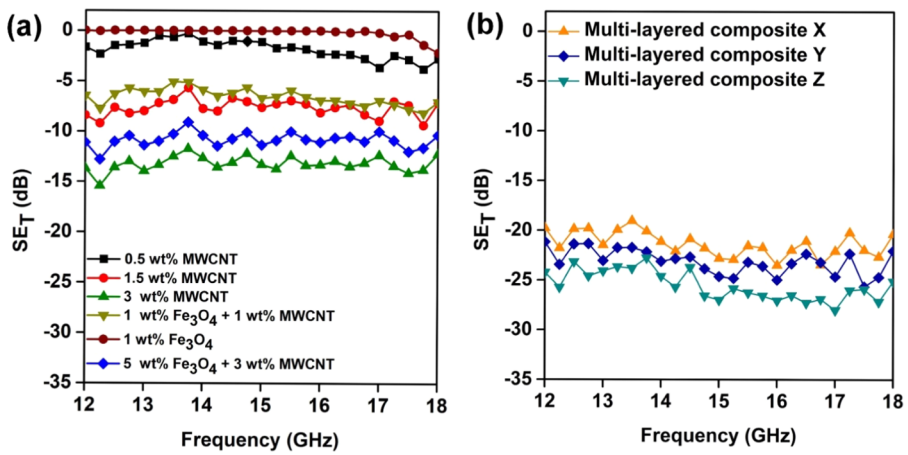

Figure 7. (a) SE_T of PDMS composites processed through spin coating. Addition of Fe_3O_4 showed zero shielding, which was due to the absence of an electrically percolated network. (b) SE_T of multilayered PDMS composites showing maximum shielding of −28 dB, i.e., blocking 99.6% of incoming EM radiation. The composition of multilayered composite films is tabulated in Table 3.

DOI: 10.1021/acsomega.8b02920
ACS Omega 2019, 4, 1781−1790

Table 5. Literature Survey of EMI Shielding PDMS Composite Thin Films

matrix	filler material	thickness (mm)	frequency (GHz)	SE_T (dB)	references
PDMS	MWCNT	2	8−12	−11	35
PDMS−PUU[a] block copolymer	MWCNT	0.7	12−18	−27	36
PDMS	Ag nanowires		8−12	−40	37
PDMS	MWCNT−graphene		8−12	−10	38
PDMS and quartz cloth	MWCNT		8−12	−16	39
PDMS multilayer	MWCNT	0.9	12−18	−26	current work
PDMS multilayer	MWCNT, Fe_3O_4	0.9	12−18	−24	current work

[a]Polyurethaneurea.

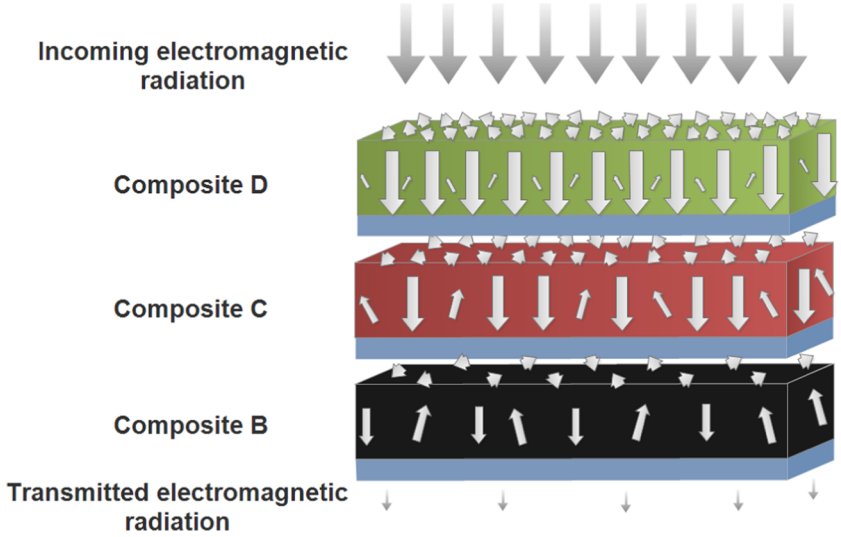

Figure 8. Schematic depicting the mechanism of EMI shielding in multilayered composites.

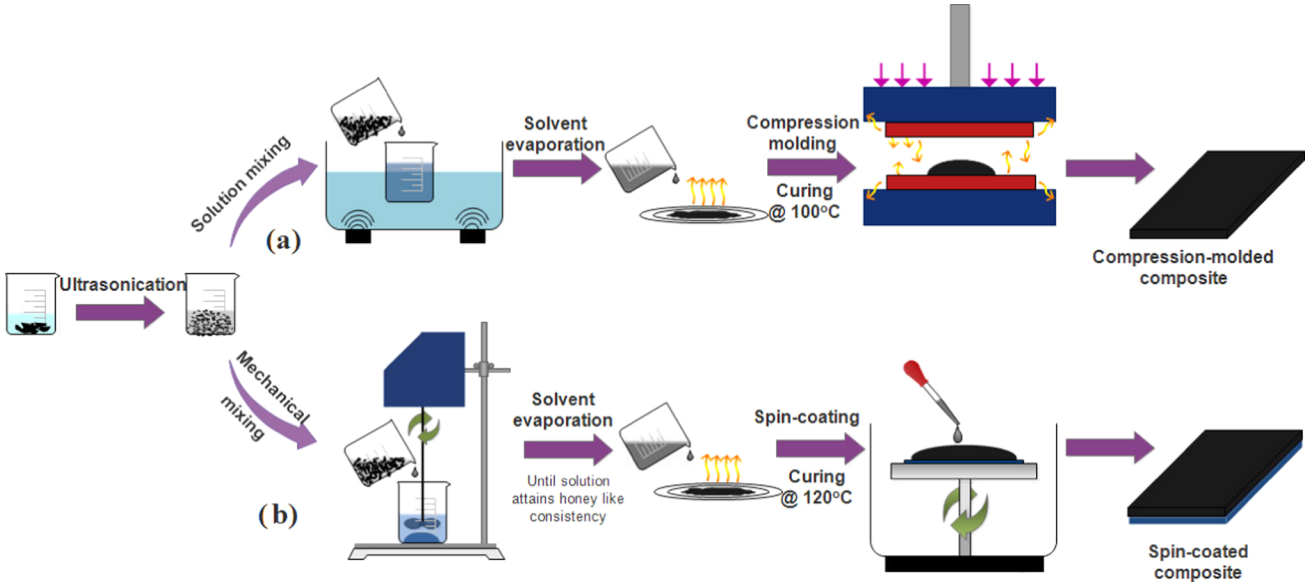

Figure 9. Schematic depicting the fabrication of PDMS composite thin films through different processing methods. (a) Compression molding and (b) spin coating.

Compression Molding. The dispersed filler solution was mixed with PDMS solution, bath sonicated for 1 h, and left under the hood for the solvent to evaporate. Curing agent was added to the composite and compression-molded at 100 °C and 10 Psi to form 150 μm composite thin film.

Spin Coating. The dispersed filler solution was mixed with PDMS using a Heidolph mechanical mixer at 300 rpm for 2 h along with Soniclean bath sonicator to remove bubbles formed during mechanical mixing. The polymer composite solution was left under the hood for the solvent to evaporate. Curing agent was added to the polymer composite solution while it retained some solvent to give the solution slightly viscous consistency. The composite solution was then poured onto a glass slide and spin-coated in a spinNXG-P1 to 150 μm thick

DOI: 10.1021/acsomega.8b02920
ACS Omega 2019, 4, 1781−1790

composite film. These PDMS composite spin-coated glass slides were cured in a hot-air oven at 120 °C for 20 min.

AUTHOR INFORMATION

Corresponding Author

*E-mail: sbose@iisc.ac.in.

ORCID

Suryasarathi Bose: 0000-0001-8043-9192

Notes

The authors declare no competing financial interest.

ACKNOWLEDGMENTS

S.S.B. and H.N. acknowledge Momentive Performance Materials Ltd., and Y.B. acknowledges Ministry of Human Resource Development (MHRD), India, for funding support.

REFERENCES

(1) Yousefi, N.; Sun, X.; Lin, X.; Shen, X.; Jia, J.; Zhang, B.; Tang, B.; Chan, M.; Kim, J. K. Highly aligned graphene/polymer nanocomposites with excellent dielectric properties for high-performance electromagnetic interference shielding. *Adv. Mater.* **2014**, *26*, 5480−5487.

(2) Zhang, Y.; Huang, Y.; Zhang, T.; Chang, H.; Xiao, P.; Chen, H.; Huang, Z.; Chen, Y. Broadband and tunable high-performance microwave absorption of an ultralight and highly compressible graphene foam. *Adv. Mater.* **2015**, *27*, 2049−2053.

(3) Chen, Z.; Xu, C.; Ma, C.; Ren, W.; Cheng, H. M. Lightweight and flexible graphene foam composites for high-performance electromagnetic interference shielding. *Adv. Mater.* **2013**, *25*, 1296−1300.

(4) IARC. *Classifies Radiofrequency Electromagnetic Fields as possible Carcinogenic to Humans*; IARC Press, 2011.

(5) Tong, X. C. *Advanced Materials and Design for Electromagnetic Interference Shielding*; CRC Press, 2016.

(6) Chung, D. D. L. Electromagnetic interference shielding effectiveness of carbin materials. *Carbon* **2001**, *39*, 279.

(7) Biswas, S.; Arief, I.; Panja, S. S.; Bose, S. Absorption-Dominated Electromagnetic Wave Suppressor Derived from Ferrite-Doped Cross-Linked Graphene Framework and Conducting Carbon. *ACS Appl. Mater. Interfaces* **2017**, *9*, 3030−3039.

(8) Biswas, S.; Panja, S. S.; Bose, S. Unique Multilayered Assembly Consisting of "Flower-Like" Ferrite Nanoclusters Conjugated with MWCNT as Millimeter Wave Absorbers. *J. Phys. Chem. C* **2017**, *121*, 13998−14009.

(9) Biswas, S.; Panja, S. S.; Bose, S. Tailored distribution of nanoparticles in bi-phasic polymeric blends as emerging materials for suppressing electromagnetic radiation: challenges and prospects. *J. Mater. Chem. C* **2018**, *6*, 3120−3142.

(10) Bhattacharjee, Y.; Bhingardive, V.; Biswas, S.; Bose, S. Construction of a carbon fiber based layer-by-layer (LbL) assembly − a smart approach towards effective EMI shielding. *RSC Adv.* **2016**, *6*, 112614−112619.

(11) Schelkunoff, S. A. *Electromagnetic Waves*; D Van Nostrand Company, Inc: London, 1943.

(12) Al-Saleh, M. H.; Sundararaj, U. Electromagnetic interference shielding mechanisms of CNT/polymer composites. *Carbon* **2009**, *47*, 1738−1746.

(13) Colaneri, N. F.; Schacklette, L. W. EMI Shielding Measurements of Conductive Polymer Blends. *IEEE Trans. Instrum. Meas.* **1992**, *41*, 291.

(14) Benhamou, S. M.; Hamouni, M.; Khaldi, S. Theoritical approach to electromagnetic shielding of multilayer conductive sheets. *Prog. Electromagn. Res.* **2015**, *41*, 9.

(15) Bhattacharjee, Y.; Arief, I.; Bose, S. Recent trends in multilayered architectures towards screening electromagnetic radiation: challenges and perspectives. *J. Mater. Chem. C* **2017**, *5*, 7390−7403.

(16) Chen, C. Y.; Chang, C. L.; Chang, C. W.; Lai, S. C.; Chien, T. F.; Huang, H. Y.; Chiou, J. C.; Luo, C. H. A low-power bio-potential acquisition system with flexible PDMS dry electrodes for portable ubiquitous healthcare applications. *Sensors* **2013**, *13*, 3077−3091.

(17) Kubo, M.; Li, X.; Kim, C.; Hashimoto, M.; Wiley, B. J.; Ham, D.; Whitesides, G. M. Stretchable microfluidic radiofrequency antennas. *Adv. Mater.* **2010**, *22*, 2749−2752.

(18) Nam, Y.; Musick, K.; Wheeler, B. C. Application of a PDMS microstencil as a replaceable insulator toward a single-use planar microelectrode array. *Biomed. Microdevices* **2006**, *8*, 375−381.

(19) Bayat, M.; Yang, H.; Ko, F.; Michelson, D.; Mei, A. Electromagnetic interference shielding effectiveness of hybrid multifunctional Fe3O4/carbon nanofiber composite. *Polymer* **2014**, *55*, 936−943.

(20) Kong, L.; Yin, X.; Yuan, X.; Zhang, Y.; Liu, X.; Cheng, L.; Zhang, L. Electromagnetic wave absorption properties of graphene modified with carbon nanotube/poly (dimethyl siloxane) composites. *Carbon* **2014**, *73*, 185−193.

(21) Langlet, R.; Lambin, P.; Mayer, A.; Kuzhir, P.; Maksimenko, S. Dipole polarizability of onion-like carbons and electromagnetic properties of their composites. *Nanotechnology* **2008**, *19*, No. 115706.

(22) Jung, J.; Lee, H.; Ha, I.; Cho, H.; Kim, K. K.; Kwon, J.; Won, P.; Hong, S.; Ko, S. H. Highly Stretchable and Transparent Electromagnetic Interference Shielding Film Based on Silver Nanowire Percolation Network for Wearable Electronics Applications. *ACS Appl. Mater. Interfaces* **2017**, *9*, 44609−44616.

(23) Bollen, P.; Quievy, N.; Detrembleur, C.; Thomassin, J. M.; Monnereau, L.; Bailly, C.; Huynen, I.; Pardoen, T. Processing of a new class of multifunctional hybrid for electromagnetic absorption based on a foam filled honeycomb. *Mater. Des.* **2016**, *89*, 323−334.

(24) Mesfin, H. M.; Hermans, S.; Huynen, I.; Delcorte, A.; Bailly, C. Thin Oriented Polymer Carbon Nanotube Composites for Microwave Absorption. *Mater. Today: Proc.* **2016**, *3*, 491−496.

(25) Monnereau, L.; Urbanczyk, L.; Thomassin, J.-M.; Pardoen, T.; Bailly, C.; Huynen, I.; Jérôme, C.; Detrembleur, C. Gradient foaming of polycarbonate/carbon nanotube based nanocomposites with supercritical carbon dioxide and their EMI shielding performances. *Polymer* **2015**, *59*, 117−123.

(26) Tran, M.-P.; Thomassin, J.-M.; Alexandre, M.; Jerome, C.; Huynen, I.; Detrembleur, C. Nanocomposite Foams of Polypropylene and Carbon Nanotubes: Preparation, Characterization, and Evaluation of their Performance as EMI Absorbers. *Macromol. Chem. Phys.* **2015**, *216*, 1302−1312.

(27) Chou, K.-S.; Huang, K.-C.; Shih, Z.-H. Effect of mixing process on electromagnetic interference shielding effectiveness of nickel/acrylonitrile-butadiene-styrene composites. *J. Appl. Polym. Sci.* **2005**, *97*, 128−135.

(28) Kasgoz, A.; Korkmaz, M.; Alanalp, M. B.; Durmus, A. Effect of processing method on microstructure, electrical conductivity and electromagnetic wave interference (EMI) shielding performance of carbon nanofiber filled thermoplastic polyurethane composites. *J. Polym. Res.* **2017**, *24*, No. 235108.

(29) Lee, S. H.; Kim, J. Y.; Koo, C. M.; Kim, W. N. Effects of processing methods on the electrical conductivity, electromagnetic parameters, and EMI shielding effectiveness of polypropylene/nickel-coated carbon fiber composites. *Macromol. Res.* **2017**, *25*, 936−943.

(30) Chen, Z.; Xu, C.; Ma, C.; Ren, W.; Cheng, H. M. Lightweight and flexible graphene foam composites for high-performance electromagnetic interference shielding. *Adv. Mater.* **2013**, *25*, 1296−1300.

(31) Danlée, Y.; Bailly, C.; Huynen, I. Thin and flexible multilayer polymer composite structures for effective control of microwave electromagnetic absorption. *Compos. Sci. Technol.* **2014**, *100*, 182−188.

(32) Danlée, Y.; Huynen, I.; Bailly, C. Thin smart multilayer microwave absorber based on hybrid structure of polymer and carbon nanotubes. *Appl. Phys. Lett.* **2012**, *100*, No. 213105.

DOI: 10.1021/acsomega.8b02920
ACS Omega 2019, 4, 1781−1790

(33) Pawar, S. P.; Biswas, S.; Kar, G. P.; Bose, S. High frequency millimetre wave absorbers derived from polymeric nanocomposites. *Polymer* **2016**, *84*, 398−419.
(34) Bose, S.; Bhattacharyya, A. R.; Kulkarni, A. R.; Pötschke, P. Electrical, rheological and morphological studies in co-continuous blends of polyamide 6 and acrylonitrile−butadiene−styrene with multiwall carbon nanotubes prepared by melt blending. *Compos. Sci. Technol.* **2009**, *69*, 365−372.
(35) Theilmann, P.; Yun, D.-J.; Asbeck, P.; Park, S.-H. Superior electromagnetic interference shielding and dielectric properties of carbon nanotube composites through the use of high aspect ratio CNTs and three-roll milling. *Org. Electron.* **2013**, *14*, 1531−1537.
(36) Ma, C.-C. M.; Huang, Y.-L.; Kuan, H.-C.; Chiu, Y.-S. Preparation and electromagnetic interference shielding characteristics of novel carbon-nanotube/siloxane/poly-(urea urethane) nanocomposites. *J. Polym. Sci., Part B: Polym. Phys.* **2005**, *43*, 345−358.
(37) Jung, J.; Lee, H.; Ha, I.; Cho, H.; Kim, K. K.; Kwon, J.; Won, P.; Hong, S.; Ko, S. H. Highly Stretchable and Transparent Electromagnetic Interference Shielding Film Based on Silver Nanowire Percolation Network for Wearable Electronics Applications. *ACS Appl. Mater. Interfaces* **2017**, *9*, 44609−44616.
(38) Kong, L.; Yin, X.; Han, M.; Yuan, X.; Hou, Z.; Ye, F.; Zhang, L.; Cheng, L.; Xu, Z.; Huang, J. Macroscopic bioinspired graphene sponge modified with in-situ grown carbon nanowires and its electromagnetic properties. *Carbon* **2017**, *111*, 94−102.
(39) Chen, M.; Zhang, L.; Duan, S.; Jing, S.; Jiang, H.; Luo, M.; Li, C. Highly conductive and flexible polymer composites with improved mechanical and electromagnetic interference shielding performances. *Nanoscale* **2014**, *6*, 3796−3803.
(40) Han, X.; Gai, L.; Jiang, H.; Zhao, L.; Liu, H.; Zhang, W. Core−shell structured Fe3O4/PANI microspheres and their Cr(VI) ion removal properties. *Synth. Met.* **2013**, *171*, 1−6.
(41) Arrigo, R.; Teresi, R.; Gambarotti, C.; Parisi, F.; Lazzara, G.; Dintcheva, N. Sonication-Induced Modification of Carbon Nanotubes: Effect on the Rheological and Thermo-Oxidative Behaviour of Polymer-Based Nanocomposites. *Materials* **2018**, *11*, 383.

DOI: 10.1021/acsomega.8b02920
ACS Omega 2019, 4, 1781−1790